RPE | Radiation Physics & Engineering
An International Peer-Reviewed Journal
Published by K.N. Toosi University of Technology
http://rpe.kntu.ac.ir
Research Article

Radiation Physics and Engineering 2021; 2(4):39–46
https://doi.org/10.22034/RPE.2022.322754.1049

Estimation of effective β-fraction of the VVER-1000 reactor in terms of exposure using DRAGON5/DONJON5

Omid Safarzadeh[a,*], Farahnaz Saadatian-Derakhshandeh[b]

[a] *Shahed University, P.O. Box: 3319118651, Tehran, Iran*
[b] *Shahid Beheshti University, P.O. Box: 1983969411, Tehran, Iran*

HIGHLIGHTS

- An efficient coupled method of predicting the kinetic parameters is developed.
- The kinetic parameters and fuel consumption are calculated during fuel burn-up.
- A systematic approach of coupled thermo-hydraulic and neutronic is used.
- The results of the coupling scheme are evaluated by KASKAD package.

ABSTRACT

The effective β-fraction has a key role in the dynamic response of the reactor. This study aims to assess the suitability and accuracy of the detailed models of DRAGON5 and DONJON5 code for estimation of the effective fraction of delayed neutron for the VVER-1000 reactor core. DRAGON5 is adopted to homogenize and condense lattice physics constants of fuel assemblies during fuel burnup, followed by DONJON5, which is used to calculate forward and adjoint flux profiles on the reactor core geometry. A thermal-hydraulic subroutine is developed for VVER-1000 reactor hollow fuel pellets to embody the reactivity feedback raised by changing the reactor power profile. The effective β-fraction is evaluated for each fissile and fertile isotopes in terms of fuel burnup. The results of the coupling scheme are evaluated using the KASKAD code package of Bushehr NPP-I (BNPP-I). The results indicate that the use of SHI and SYBILT modules of DRAGON5 are essential to achieve reasonably precise resolution.

KEYWORDS

Delayed neutron fraction
VVER-1000
Burnup
DRAGON5
DONJON5

HISTORY

Received: 2 January 2022
Revised: 2 February 2022
Accepted: 21 February 2022
Published: Autumn 2021

1 Introduction

A decay of the specified fission products with large enough excess neutrons is known as β-delayed neutron emission. Although, these neutrons comprise less than 1% of total neutron released by fission reaction, delayed neutrons are more attributable to the multiplication since their energy spectrum is softer than the prompt ones (Keepin, 1965). It is of primary importance to accurately calculate the effective β-fraction for control of the reactor power. Therefore, the measurement (Agramunt et al., 2016; Rudstam et al., 2002) and calculation (Yamanaka, 2021; Kheradmand Saadi and Abbaspour, 2017) of delayed β-fraction are treated by several researchers. The methods of measuring effective β-fraction is categorized by semiemparical, reactivity substitution, and noise techniques. DRAGON/DONJON is especially submitted in the evaluation of several parameters of the CANDU reactor (Varin and Marleau, 2006; Zadeh et al., 2017).

In this context, the aim of the present study is to assess the suitability and accuracy of the detailed models of DRAGON5 and DONJON5 code for the evaluation of the effective fraction of delayed neutron for the VVER-1000 reactor core. We used DRAGON5 to homogenize and condense the cross-sections of hexagonal fuel assemblies. Then, the adjoint flux profile is computed using diffusion theory on the simple heterogeneous core using DONJON5.

The thermal-hydraulic conditions are reflected on lattice physics constants by the establishment of a coupling scheme to represent the mathematical model of the VVER-1000 reactor core. A consistent set of continuum equations for the conservation of mass, momentum, and energy of two-phase homogeneous fluid is used. The effective β-fraction of the reactor core is inconstant since the composition of the fuel rod is altering by burnup as the fer-

*Corresponding author: safarzadeh@shahed.ac.ir

tile and fissile isotopes with different values of β-fractions are generated. Furthermore, the effective β-fraction is pertinent to the prompt and delayed leakages, which are affected by the reactor core arrangement as well as by the control rod position. In this paper, the contribution of the fissile and fertile isotopes to effective β-fraction is also disclosed concerning the burnup values for the VVER-1000 reactor from the beginning of cycle (BOC) to the end of cycle (EOC). The yield and fission spectrum of delayed neutrons are used for determining the effective β-fraction by use of adjoint flux as the weighted diffusion (Henry et al., 1977). The results of the coupling scheme are evaluated using the KASKAD code package of BNPP-I (AEOI, 2006).

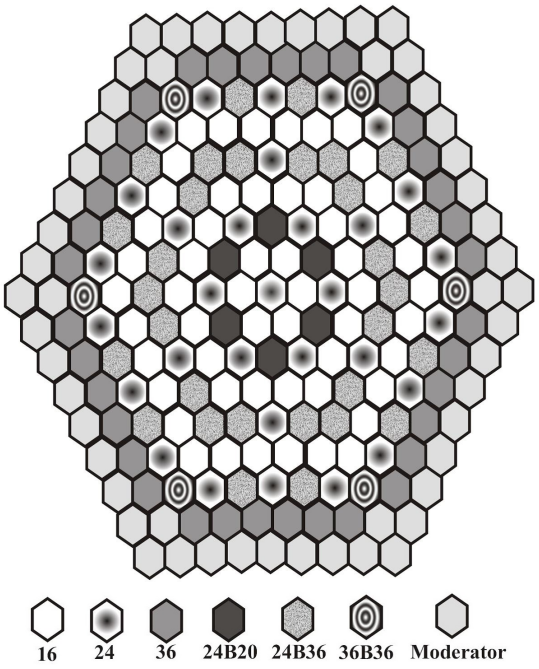

Figure 1: Control rod bank locations.

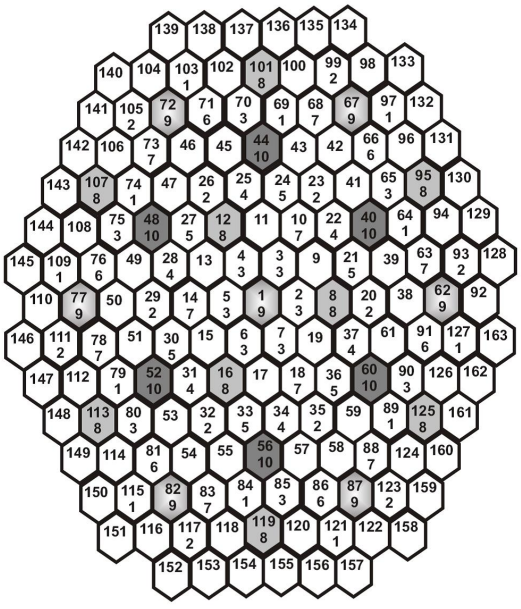

Figure 2: Modeling of the reactor core.

2 The reactor core arrangement

BNPP-I is a VVER-1000 type reactor in which the core is loaded with 163 hexagonal assemblies. Table 1 gives the details of the six diverse kinds of fuel assemblies at the first cycle loading pattern. The reactor core arrangement and the location of the control rod banks are depicted in Figs. 1 and 2, respectively. The safety and control of the reactor are accomplished by the use of ten control groups. The control rod is composed of two types of materials: the first ten percent is composed of $Dy_2O_3TiO_2$, and the rest ninety percent is made of B_4C. The fuel assembly configuration is comprised of water tube, fuel rods, instrumentation tube, and guide tubes, as shown in Fig. 3. The operating parameters of the BNPP-I is described in Table 2.

Table 1: VVER-1000 fuel assembly description.

Type	Number of fuel rods (enrichment, %)		Number of burnable rods (Boron content, g.cm^{-3})
	Fuel rod type 1	Fuel rod type 2	
16	311 (1.6)	-	-
24	311 (2.4)	-	-
36	245 (3.7)	66 (3.3)	-
24B20	311 (2.4)	-	18 (0.020)
24B36	311 (2.4)	-	18 (0.036)
36B36	245 (3.7)	66 (3.3)	18 (0.036)

Table 2: Some of thermal-hydraulic parameters of the BNPP-I reactor.

Parameter	Value
Thermal power (MW)	3000
The coolant pressure at the hot leg (MPa)	15.7
Vessel pressure differential (MPa)	0.381
Coolant velocity at core inlet (m.s^{-1})	5.6
Total coolant ow rate (m^2.h^{-1})	84800
Core flow area (m^2)	4.14

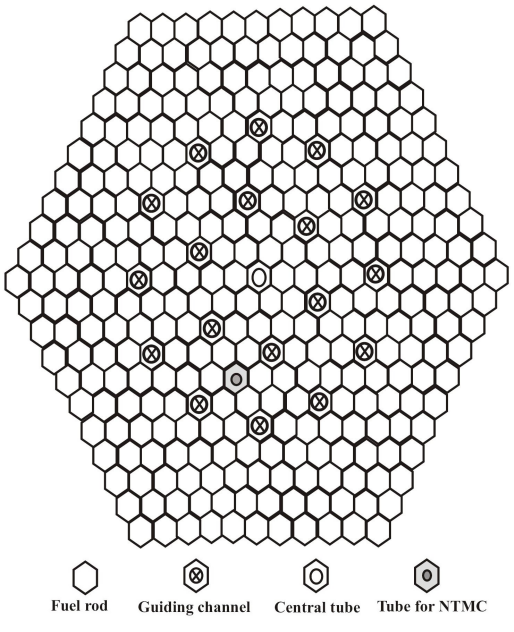

Figure 3: VVER-1000 Fuel assembly.

3 Lattice physics constants and core flux profile

Neutronic computation is frequently accomplished in two steps for practical purposes. In the first step, the transport equation with resonance self-shielding and leakage treatments is used over the assemblies using reflective boundary conditions to form condensed cross-sections and diffusion library of the fuel assembly. In the second step, the generated group constants are used to simply model the whole core that is treated by diffusion theory.

We used DRAGON5 to represent the fuel assemblies in exact geometry during the operating cycle and to create homogenized cross-sections. The resonance self-shielding is considered by the SHI module where Stamm'ler method (Stammler and Abbate, 1983) was implemented, and the transport equation is solved by the collision probability method, which is realized by the SYBILT module. The isotopic depletion chain and the microscopic cross-sections are extracted from the DRAGON library in *DRAGLIB* format with 295 energy groups (Hébert, 2016; Marleau et al., 2011). The leakage between the fuel assembly and surrounding domains is clearly considered by employing the B_1 leakage model. The critical spectrum is used to generate the few group constants for assemblies placed on the core periphery.

In the next step, these data are used in DONJON5 to determine the forward-, adjoint-flux profiles on simple heterogeneous core (Hébert, 2016; Hébert et al., 2018). The active core is axially discretized into 10 layers plus two more layers for capturing the upper and lower reflectors. A mesh-centered finite difference method in the hexagonal geometry of the reactor core is used to provide the numerical solution of the diffusion equation.

4 Thermal-hydraulic calculation

A thermal-hydraulic subroutine for the VVER-1000 reactor, which contains hollow fuel pellets, is developed to embody the reactivity feedback raised by changing the reactor power profile. In this subroutine, the heated channel model is used to model the thermal-hydraulic behavior of the fuel assembly (Todreas et al., 2021; Safarzadeh et al., 2015).

The mass, momentum, and energy conservation equations in one-dimensional flow are written as (Todreas et al., 2021):

$$\frac{\partial(\rho A_z)}{\partial t} + \frac{\partial(\rho v A_z)}{\partial z} = 0 \tag{1}$$

$$\frac{\partial}{\partial t}(\rho v A_z) + \frac{\partial}{\partial z}(\rho v^2 A_z) = -\frac{\partial(\rho A_z)}{\partial z} - \int_{\rho_z} \tau \, \mathrm{d}P_z - \rho g A_z \tag{2}$$

$$\rho \frac{\partial h}{\partial t} + \rho v \frac{\partial h}{\partial z} = \frac{\partial p}{\partial t} + \frac{\dot{q}'' P_h}{A_z} + \frac{\rho v}{\rho}\left(\frac{\partial p}{\partial z} + \frac{f \rho^2 v |v|}{2 \rho D_e}\right) \tag{3}$$

with ρ as fluid density, v as velocity of the fluid, A_z as the cross-sectional area of the channel, p as fluid pressure, τ as shear stress, g as gravity constant, h as fluid enthalpy, $\dot{q}''$ as heat flux rate, P_h as heated perimeter, f as friction factor, and D_e is hydraulic equivalent diameter. These equations are solved to determine fluid temperature and pressure using the finite volume method. The heat generated from the fuel is transferred to the fluid by the coupled convection and conduction heat transport modes. Therefore, the surface temperature of clad and fuel can be calculated using formerly obtained fluid temperature as:

$$T_c^{out} - T_b = \frac{\dot{q}'}{2\pi R_c o h} \tag{4}$$

$$T_c^{in}(z) = \frac{\dot{q}'(z)}{2\pi k_c} \ln\left(\frac{R_{co}}{R_{ci}}\right) + T_c^{out}(z) \tag{5}$$

$$T_f^{out} = \frac{\dot{q}''}{h_g} + T_c^{in} \tag{6}$$

$$\bar{k_f}(T_f^{in} - T_f^{out}) = \frac{\dot{q}''' R_{f_o}^2}{4} \times \left\{1 - \left(\frac{R_{f_i}}{R_{f_o}}\right)^2 - \left(\frac{R_{f_i}}{R_{f_o}}\right)^2 \ln\left(\frac{R_{f_o}}{R_{f_i}}\right)^2\right\} \tag{7}$$

where T_b is the bulk fluid temperature, T_c^{out} is the clad temperature at the outer surface, h is the convective heat transfer coefficient, $\dot{q}'$ is the linear heat source, R_{co} is the clad outer radius, k_c is the clad thermal conductivity, R_{ci} is the inner radius of the clad, T_f^{out} is outer fuel temperature, g_p is gap conductance, T_c^{in} is clad inner surface temperature, T_f^{in} is inner fuel temperature, $\bar{k_f}$ is the average thermal conductivity of the fuel, R_{f_o} is fuel outer radius, R_{f_i} is inner fuel radius, and $\dot{q}'''$ is the volumetric heat source.

5 Effective β-fraction

A decay of the specified fission products with a large enough excess neutrons is known as -delayed neutron emission. The six groups of delayed neutron emitters are generally accepted in reactor kinetics studies. The effective β-fraction in the i^{th} precursor group is defined as the fraction of delayed neutrons that appeared in that group as (Ott and Bezella, 1983):

$$\beta_i(t) = \frac{\int \mathrm{d}V \int \mathrm{d}E \, W(r,E) \sum_j \chi_i \beta_i^j F^j \Phi(r,E,t)}{\int \mathrm{d}V \int \mathrm{d}E \, W(r,E) \sum_j \chi^j F^j \Phi(r,E,t)} \tag{8}$$

where $i = 1, 2, ..., 6$, $W(r,E)$ is a weight function, $\Phi(r,E,t)$ is the neutron flux density, β_i^j is the physical fraction of the delayed neutrons emitted from a fissionable isotope j that eventually appears from the decay of precursor i, χ_i is the spectrum of emission energies for the i^{th} precursor, χ^j is prompt neutron spectrum of isotope j, and F^j is an operator at point r and time t as:

$$F^j f = \int_0^\infty \nu \Sigma_f^j(r,E',t) f(r,E',t) \, \mathrm{d}E' \tag{9}$$

where $f(r,E,t)$ is an arbitrary function, and $\nu\Sigma_f^j$ is production cross-section from isotope j. The total effective

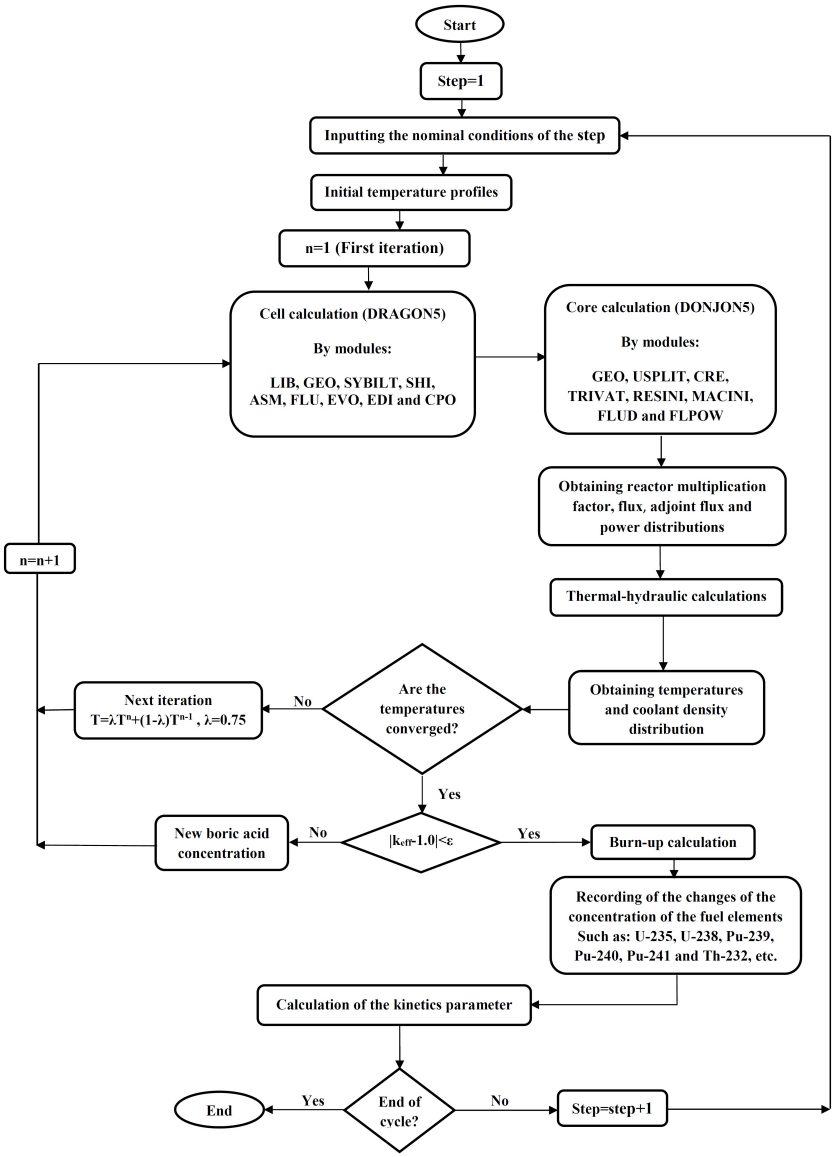

Figure 4: Flow chart of the effective β-fraction calculation.

β-fraction can be obtained as:

$$\beta_{\text{eff}}(t) = \sum_{i=1}^{I} \beta_i(t) \tag{10}$$

The adjoint flux is recommended by many authors as the weighting function to obtain a good estimation of the problem at the expense of complexities (Henry et al., 1977). Therefore, the effective β-fraction can be obtained as:

$$\beta_{\text{eff}} = \frac{\sum_j V_j \sum_g \chi'_{i,g}\varphi^*_{i,g} \sum_b \beta_{b,i} N_{b,j} \sum_{g'} \nu\sigma_{f,g',b,j}\varphi_{j,g'}}{\sum_j V_j \sum_g \chi_g \varphi^*_{i,g} \sum_{g'} \nu\Sigma_{f,g'}\varphi_{j,g'}} \tag{11}$$

where $\beta_{b,i}$ refers to the delayed neutron fraction of delayed family i, $N_{b,j}$ is the atomic density at location j for nuclide b, $\chi'_{i,g}$ is the delayed neutron spectrum, χ_g is prompt neutron distribution function, and φ and φ^* is the forward and the adjoint ux shapes, respectively. Also, g and g' are energy group index, ν is the average number of neutrons released per ssion, and V_j is volume at the location j. Furthermore, σ_f and Σ_f refer to microscopic and macroscopic ssion cross-section, respectively.

6 Calculation procedure

The calculation scheme for assessing the effective β-fraction has been depicted in Fig. 4. The basic structure consists of the following steps:

1. The required input data such as initial boric acid concentration, operating time interval, thermal power, the rod bank situation, and initial temperature profiles are set.

2. DRAGON5 is utilized to compute the coarse group cross-sections and diffusion coefficient for fuel assemblies. The equivalent group constants are transformed to a consistent format that can be read by DONJON5 using CPO module.

3. The reactor core is simulated in DONJON5. The axial direction of the fuel assembly is split to ten layers. The reflectors are modeled by three zones at upper, lower and lateral side of the active core. The CRE module is utilized to interpolate the cross-sections produced by the DRAGON5.

4. The coolant temperature distributions in the reactor core are determined by developed VVER-1000 thermal-hydraulic subroutine.

5. The fuel temperature is used as a convergence criterion.

6. The concentration of the fuel elements during the operating burnup cycle in the whole regions of the reactor core is done through EVO module of DRAGON5.

7. The effective delayed neutron fraction is computed.

8. The termination of the cycle is checked. If the criterion is not satisfied, the process is repeated through the last burnup step data from step 2.

7 Results

The proposed approach is used to compute the effective β-fraction in the VVER-1000 reactor. The nominal operational parameters are used to model the kinetic parameter evolution. Table 3 describes these parameters during the operating cycle.

Figures 5 and 6 illustrate the mass fraction variations of the U-235 and U-238 isotopes in the six fuel assemblies composing the reactor during the first fuel cycle. The changes of the mass of fissionable isotopes Pu-239, Pu-240, and Pu-241 in the reactor core in terms of the burnup values illustrate in Fig. 7.

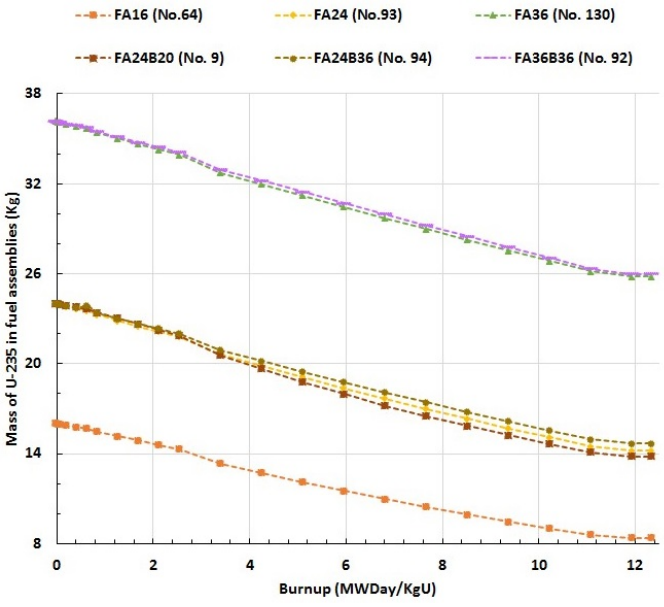

Figure 5: The mass change of the U-235 isotope in terms of burnup.

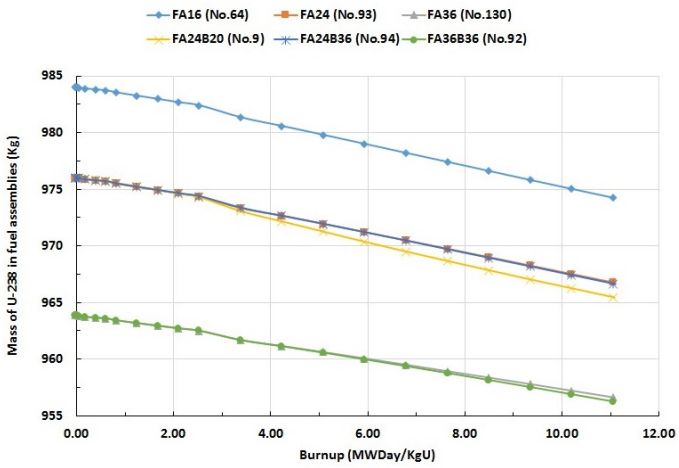

Figure 6: The mass change of the U-238 isotope in terms of burnup.

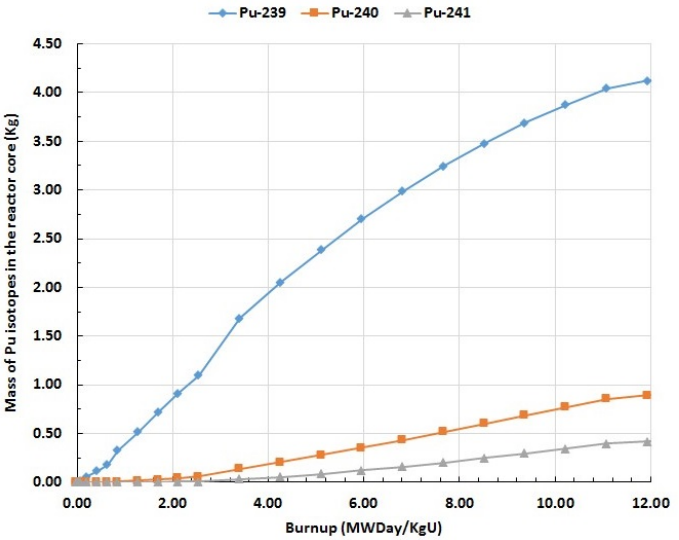

Figure 7: The mass change of the Pu isotopes in terms of burnup.

The effective β-fraction is represented during the first fuel cycle of the VVER-1000 reactor and compared with those existing in the plant's FSAR (AEOI, 2007). The results of adopted scheme are shown in Table 4 in comparison with the reference solution. The average error is about 1.33%. The results show a suitable agreement. A sensitivity study is also done for the mesh splitting. It is revealed that the effective β-fraction does not change significantly by fuel assembly mesh.

The contribution of effective β-fraction from fissionable isotopes is shown in Table 5. As can be seen, the effective β-fraction of U-235 decreases with fuel burnup while the contribution of effective β-fraction from U-238, Pu-239, Pu-240, and Pu-241 is increased. Pu-241 has a negligible effect on effective delayed neutron fraction. The group-wise effective β-fraction is also calculated and presented in Table 6.

Table 3: The first cycle nominal operating condition. In this table, H_{10} shows the percentage of 10^{th} control bank outage, and C_{bc} is the concentration of the critical boric acid.

Effective operational days	Inlet coolant temperature (°C)	H_{10}(%)	Reactor power (MW)	C_{bc} (g.kg^{-1})
0.00	280.5	60	150	6.90
0.10	282.8	60	750	6.12
1.00	282.8	60	750	6.07
2.00	284.4	70	1200	5.74
5.00	284.4	70	1200	5.61
10.00	285.5	80	1500	5.36
15.00	285.5	80	1500	5.31
20.00	288.3	80	2250	4.94
30.00	288.3	80	2250	4.86
40.00	288.3	80	2250	4.75
50.00	288.3	80	2250	4.62
60.00	288.3	80	2700	4.49
70.00	289.9	80	2850	4.16
75.00	290.5	90	2850	4.03
80.00	290.5	90	3000	3.98
100.00	291.0	90	3000	3.58
120.00	291.0	90	3000	3.22
140.00	291.0	90	3000	2.86
160.00	291.0	90	3000	2.49
180.00	291.0	90	3000	2.11
200.00	291.0	90	3000	1.73
220.00	291.0	90	3000	1.34
240.00	291.0	90	3000	0.96
260.00	291.0	90	3000	0.57
280.00	291.0	90	3000	0.19
289.71	291.0	90	3000	0.00

Table 4: Sensitivity analysis of effective β-fraction during the first cycle of the VVER-1000 reactor. Here, n is the hexagonal mesh, and n=2, 3, and 4 means the hexagon divided into 6, 24, and 54 triangles, respectively.

Effective	FSAR	Our results (%)		
operational days	(%)	n=2	n=3	n=4
0.00	0.74	0.7462	0.7462	0.7461
0.10	0.74	0.7463	0.7463	0.7462
1.00	0.74	0.7471	0.7471	0.7469
2.00	0.74	0.7466	0.7466	0.7464
5.00	0.74	0.7443	0.7442	0.7441
10.00	0.73	0.7406	0.7409	0.7408
15.00	0.73	0.7370	0.7367	0.7366
20.00	0.72	0.7275	0.7280	0.7279
30.00	0.71	0.7161	0.7158	0.7157
40.00	0.70	0.7050	0.7040	0.7040
50.00	0.70	0.6931	0.6926	0.6927
60.00	0.69	0.6811	0.6805	0.6806
70.00	0.68	0.6786	0.6789	0.6790
75.00	0.67	0.6749	0.6747	0.6748
80.00	0.67	0.6508	0.6511	0.6512
100.00	0.66	0.6359	0.6359	0.6361
120.00	0.64	0.6245	0.6240	0.6242
140.00	0.63	0.6126	0.6122	0.6124
160.00	0.62	0.5996	0.5992	0.5994
180.00	0.60	0.5908	0.5905	0.5907
200.00	0.60	0.5857	0.5855	0.5859
220.00	0.59	0.5732	0.5731	0.5734
240.00	0.58	0.5683	0.5683	0.5688
260.00	0.57	0.5605	0.5608	0.5612
280.00	0.56	0.5583	0.5586	0.5591
289.71	0.55	0.5588	0.5592	0.5597

8 Conclusions

This paper is devoted to the qualification of an important kinetic parameter for VVER-1000 reactor using DRAGON5/DONJON5. The results indicate that the SHI and SYBILT modules can be used for proving the accuracy of effective β-fraction. At BOC, the delayed fraction is about 0.007462 and decreases to 0.005588 at EOC. The contribution of the effective β-fraction is 84% for 235U and against 16% for 238U at BOC which goes to the level of 56% for 235U, 23% for U-238, 16% for Pu-239 and 5% for Pu-241 at EOC. The coupled method leads to precise prediction of the effective β-fraction. The error in effective β-fraction about its average is only ± 0.01. The results accuracy is changed with increasing the hexagonal mesh splitting to 54 triangles (n=4), but it is not negligible.

References

AEOI (2006). *Album of Neutron and Physical Characteristics of the initial fuel inventory. Organization of operation on BNPP-1.* Atomic Energy Organization of Iran.

AEOI (2007). *Final Safety Analysis Report.* Atomic Energy Organization of Iran.

Agramunt, J., Tain, J., Gómez-Hornillos, M. B., et al. (2016). Characterization of a neutron–beta counting system with beta-delayed neutron emitters. *Nuclear Instruments and Methods in Physics Research Section A: Accelerators, Spectrometers, Detectors and Associated Equipment*, 807:69–78.

Table 5: Contribution to delayed neutron fraction from each ssionable nuclide.

Effective operational days	U-235	U-238	Pu-239	Pu-240	Pu-241
0.00	0.628427	0.117761	0	0	0
0.10	0.628313	0.117949	0.000007	0	0
1.00	0.627399	0.119702	0.000051	0	0
2.00	0.625991	0.120218	0.000434	0	0
5.00	0.621337	0.121118	0.001821	0	0
10.00	0.616091	0.120942	0.003559	0	0.000001
15.00	0.608952	0.122311	0.005689	0	0.000005
20.00	0.594400	0.122660	0.010385	0.000001	0.000023
30.00	0.574697	0.124841	0.016468	0.000003	0.000099
40.00	0.557448	0.125379	0.021968	0.000006	0.000236
50.00	0.539576	0.125301	0.027721	0.000009	0.000469
60.00	0.521638	0.125207	0.033440	0.000013	0.000838
70.00	0.518343	0.124716	0.034543	0.000014	0.000948
75.00	0.509421	0.127254	0.036983	0.000017	0.001199
80.00	0.473060	0.126672	0.048291	0.000029	0.002778
100.00	0.448452	0.127284	0.055487	0.000041	0.004602
120.00	0.428101	0.128659	0.061138	0.000053	0.006538
140.00	0.409336	0.128096	0.066463	0.000065	0.008687
160.00	0.387784	0.127788	0.072372	0.000080	0.011539
180.00	0.372336	0.127926	0.076371	0.000092	0.014034
200.00	0.362009	0.128853	0.078858	0.000101	0.015857
220.00	0.342532	0.126991	0.083921	0.000118	0.019671
240.00	0.332045	0.127847	0.086269	0.000129	0.021981
260.00	0.319309	0.126658	0.089306	0.000143	0.025127
280.00	0.314479	0.126929	0.090319	0.000149	0.026395
289.71	0.315511	0.126828	0.090047	0.000148	0.026271

Table 6: The group-wise delayed neutron fraction.

Effective	$\beta_{\text{eff},i}$ (%)						β_{eff} (%)
operational days	1	2	3	4	5	6	
0.00	0.02364	0.12684	0.12384	0.28842	0.12956	0.05389	0.7462
0.10	0.02364	0.12684	0.12385	0.28845	0.12959	0.05390	0.7463
1.00	0.02363	0.12688	0.12393	0.28879	0.12990	0.05402	0.7472
2.00	0.02361	0.12678	0.12382	0.28857	0.12987	0.05400	0.7467
5.00	0.02351	0.12637	0.12338	0.28757	0.12960	0.05386	0.7443
10.00	0.02338	0.12581	0.12277	0.28604	0.12902	0.05358	0.7406
15.00	0.02323	0.12518	0.12210	0.28450	0.12860	0.05335	0.7370
20.00	0.02290	0.12370	0.12047	0.28055	0.12718	0.05267	0.7275
30.00	0.02246	0.12184	0.11846	0.27578	0.12566	0.05190	0.7161
40.00	0.02206	0.12012	0.11656	0.27116	0.12403	0.05110	0.7050
50.00	0.02165	0.11829	0.11453	0.26618	0.12220	0.05022	0.6931
60.00	0.02124	0.11648	0.11250	0.26121	0.12038	0.04934	0.6812
70.00	0.02116	0.11611	0.11208	0.26014	0.11994	0.04913	0.6786
75.00	0.02097	0.11542	0.11134	0.25855	0.11963	0.04895	0.6749
80.00	0.02013	0.11182	0.10725	0.24851	0.11596	0.04716	0.6508
100.00	0.01957	0.10955	0.10463	0.24222	0.11380	0.04609	0.6359
120.00	0.01912	0.10780	0.10259	0.23741	0.11227	0.04530	0.6245
140.00	0.01869	0.10609	0.10054	0.23243	0.11048	0.04442	0.6127
160.00	0.01819	0.10421	0.09825	0.22690	0.10856	0.04345	0.5996
180.00	0.01785	0.10294	0.09667	0.22316	0.10732	0.04282	0.5908
200.00	0.01762	0.10218	0.09572	0.22098	0.10670	0.04248	0.5857
220.00	0.01717	0.10050	0.09357	0.21572	0.10476	0.04152	0.5732
240.00	0.01694	0.09978	0.09262	0.21357	0.10417	0.04119	0.5683
260.00	0.01664	0.09877	0.09126	0.21028	0.10299	0.04059	0.5605
280.00	0.01654	0.09846	0.09083	0.20929	0.10272	0.04044	0.5583
289.71	0.01656	0.09854	0.09093	0.20952	0.10278	0.04047	0.5588

Hébert, A. (2016). DRAGON5 and DONJON5, the contribution of École Polytechnique de Montréal to the SALOME platform. *Annals of Nuclear Energy*, 87:12–20.

Hébert, A., Sekki, D., and Chambon, R. (2018). A user guide for DONJON Version5. Institut de génie nucléaire, Département de génie mécanique, École Polytechnique de Montréal. Montréal, QC. Technical report, Canada, Tech. Rep. IGE-344.

Henry, A. F., Scott, C., and Moorthy, S. (1977). Nuclear reactor analysis. *IEEE Transactions on Nuclear Science*, 24(6):2566–2567.

Keepin, G. R. (1965). *Physics of Nuclear kinetics*. Addison-Wesley Publishing Company.

Kheradmand Saadi, M. and Abbaspour, A. (2017). Effective point kinetic parameters calculation in tehran research reactor using deterministic and probabilistic methods. *Nuclear Science and Techniques*, 28(12):1–11.

Marleau, G., Hébert, A., and Roy, R. (2011). A user guide for DRAGON Version 4. *Institute of Genius Nuclear, Department of Genius Mechanical, School Polytechnic of Montreal*.

Ott, K. O. and Bezella, W. A. (1983). *Introductory nuclear reactor statics*. Amer Nuclear Society.

Rudstam, G., Finck, P., Filip, A., et al. (2002). Delayed neutron data for the major actinides. *A report by the Working Party on International Evaluation Co-operation of the OECD NEA Nuclear Science Committee*, 6.

Safarzadeh, O., Saadatian-Derakhshandeh, F., and Shirani, A. (2015). Calculation of reactivity coefficients with burn-up changes for VVER-1000 reactor. *Progress in Nuclear Energy*, 81:217–227.

Stammler, R. J. and Abbate, M. J. (1983). Methods of steady-state reactor physics in nuclear design.

Todreas, N. E., Kazimi, M. S., and Massoud, M. (2021). *Nuclear systems Volume II: Elements of thermal hydraulic design*. CRC Press.

Varin, E. and Marleau, G. (2006). Candu reactor core simulations using fully coupled DRAGON and DONJON calculations. *Annals of Nuclear Energy*, 33(8):682–691.

Yamanaka, M. (2021). Effective delayed neutron fraction. In *Accelerator-Driven System at Kyoto University Critical Assembly*, pages 83–123. Springer, Singapore.

Zadeh, F. M., Etienne, S., Chambon, R., et al. (2017). Effect of 3-D moderator flow configurations on the reactivity of CANDU nuclear reactors. *Annals of Nuclear Energy*, 99:136–150.